Cryogenian glaciostatic and eustatic fluctuations and massive Marinoan-related deposition of Fe and Mn in the Urucum District, Brazil

B.T. Freitas[1], I.D. Rudnitzki[2], L. Morais[3,4], M.D.R. Campos[1], R.P. Almeida[3], L.V. Warren[5], P.C. Boggiani[3], S. Caetano-Filho[3], C. Bedoya-Rueda[3], M. Babinski[3], T.R. Fairchild[3] and R.I.F. Trindade[4]

[1]Faculdade de Tecnologia, Universidade de Campinas, Limeira, SP 13484-332, Brazil
[2]Departamento de Geologia, Universidade Federal de Ouro Preto, Ouro Preto, MG 35400-000, Brazil
[3]Instituto de Geociências, São Paulo, SP 05508-080, Brazil
[4]Instituto de Astronomia, Geofísica e Ciências Atmosféricas, Universidade de São Paulo, São Paulo, SP 05508-090, Brazil
[5]Departamento de Geologia, Universidade Estadual Paulista, Rio Claro, SP 13506-900, Brazil

ABSTRACT

Global Neoproterozoic glaciations are related to extreme environmental changes and the reprise of iron formation in the rock record. However, the lack of narrow age constraints on Cryogenian successions bearing iron-formation deposits prevents correlation and understanding of these deposits on a global scale. Our new multiproxy data reveal a long Cryogenian record for the Jacadigo Group (Urucum District, Brazil) spanning the Sturtian and Marinoan ice ages. Deposition of the basal sequence of the Urucum Formation was influenced by Sturtian continental glaciation and was followed by a transgressive interglacial record of >600 m of carbonates that terminates in a glacioeustatic unconformity. Overlying this, there are up to 500 m of shale and sandstone interpreted as coeval to global Marinoan glacial advance. Glacial outwash delta deposits at the top of the formation correlate with diamictite-filled paleovalleys and are covered by massive Fe and Mn deposits of the Santa Cruz Formation and local carbonate. This second transgression is related to Marinoan deglaciation. Detrital zircon provenance supports glaciostatic control on Cryogenian sedimentary yield at the margins of the Amazon craton. These findings reveal the sedimentary response to two marked events of glacioeustatic incision and transgression, culminating in massive banded iron deposition during the Marinoan cryochron.

INTRODUCTION

The reappearance of iron formation (IF) in the Neoproterozoic after more than 1 b.y. is one of the main tenets of the snowball Earth hypothesis (e.g., Cox et al., 2013). Evidence for two global glacial intervals in the late Neoproterozoic is now precisely constrained between ca. 717 Ma and 658 Ma for the Sturtian cryochron and between ca. 645 Ma and 635 Ma for the Marinoan cryochron (Cox et al., 2018; Zhou et al., 2019; Nelson et al., 2020; Rooney et al., 2020). However, Cryogenian IF deposits are either demonstrably Sturtian or lack precise age constraints, suggesting a possible genetic synchronicity related to metal sourcing from late Tonian large igneous provinces (Cox et al., 2013, 2016, and references therein [both papers]). The Jacadigo Group in central South America comprises the largest Neoproterozoic IF in the world,

with 36 Gt of Fe ore reserves over an impressive stratigraphic thickness of ∼350 m, dominated by high-grade banded IF. Yet, its sedimentary context and age are still debated (Urban et al., 1992; Freitas et al., 2011; Angerer et al., 2016).

We present a novel stratigraphic framework for the Jacadigo Group supported by new sedimentological and geochemical data. Our results integrate the Jacadigo Group record into the recently defined Cryogenian time frame as a key case history of Cryogenian glacioeustatic base-level fluctuations that culminated in the largest Fe and Mn sedimentary deposits of the Neoproterozoic.

GEOLOGIC SETTING

The Jacadigo Group consists of the Urucum and Santa Cruz Formations (Fig. 1; de Almeida, 1946). In the up to 1-km-high hills of the

Urucum District (UD) in Brazil, the Jacadigo Group sits upon basement rocks of the Rio Apa block, dominated by 1900–1700 Ma granites and gneisses (Fig. 1; Redes et al., 2015; McGee et al., 2018). The Urucum Formation was previously described as a dominantly siliciclastic succession hundreds of meters thick, starting with coarse-grained deposits, followed by arkose, shale, and local carbonate beds (Freitas et al., 2011; Angerer et al., 2016). This passes upward to the Santa Cruz Formation, comprising more than 300 m of high-grade IF with minor Mn-rich beds and siliciclastic intercalations (de Almeida, 1946; Urban et al., 1992).

The Jacadigo Group has been interpreted as the sedimentary response to extensional tectonics at the margins of the Amazon craton, either in a divergent plate setting (Freitas et al., 2011) or in a convergent setting (Trompette et al., 1998; Angerer et al., 2016), mostly due to supposed abrupt thickness variations between the UD center and its surroundings. The Urucum Formation has been interpreted as alluvial with subordinate lacustrine deposits, based on the dominance of sandy coarse-grained facies and abundant cross-strata in previously described outcrops (Freitas et al., 2011, and references therein). The Santa Cruz Formation has been ascribed to a restricted marine environment under glacial influence, as suggested by the presence of outsized lonestones (Urban et al., 1992; Angerer et al., 2016; for alternative interpretations, see Freitas et al., 2011).

Previous U-Pb detrital zircon geochronology pointed to a maximum depositional age of 1325 ± 24 Ma for the Urucum Formation (McGee et al., 2018) and a maximum age of 695 ± 17 Ma for the Santa Cruz Formation
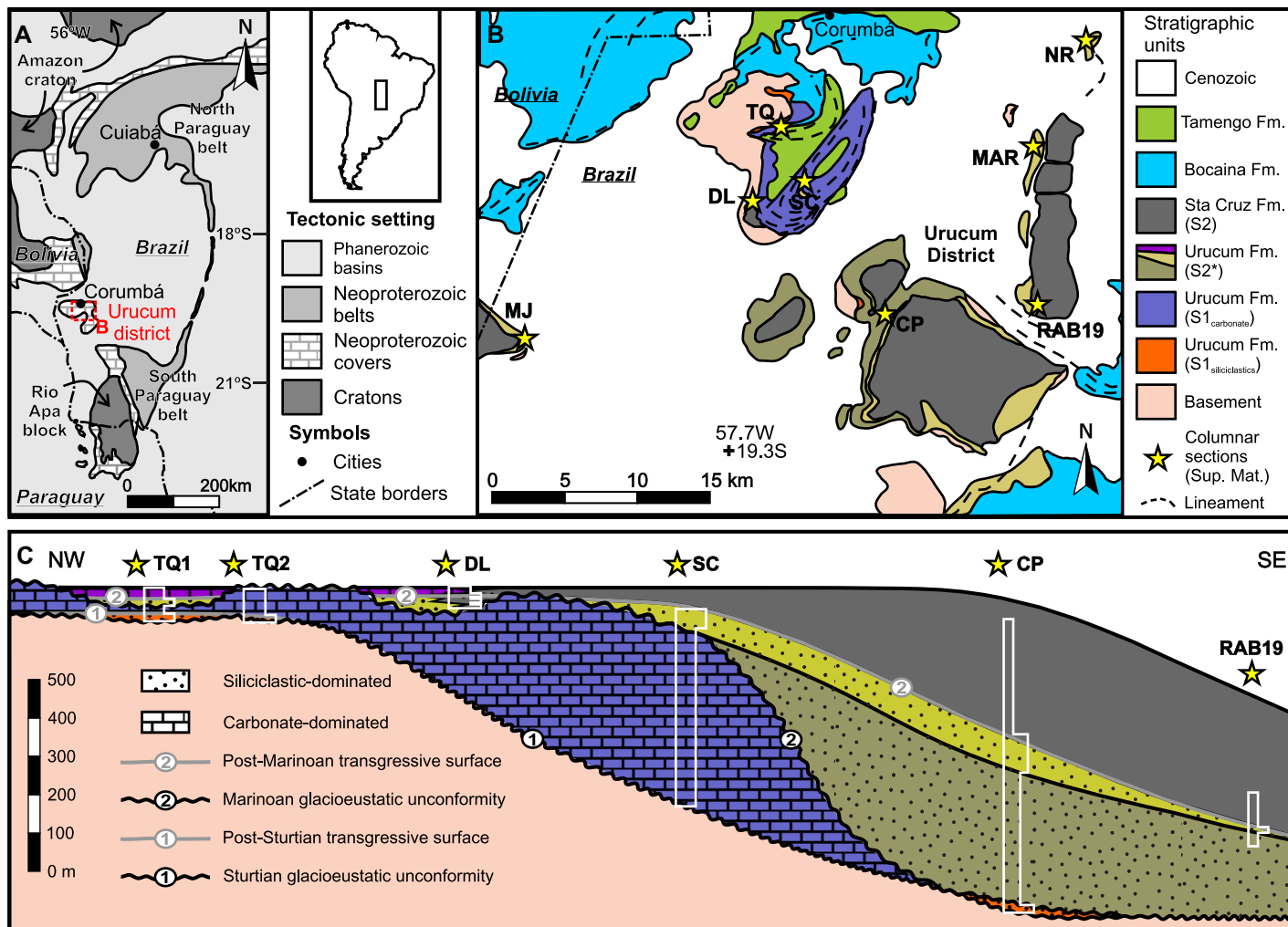
Figure 1. (A) Geological setting, (B) sketch map, and (C) sequence stratigraphic framework of studied deposits. (S2*) Color scheme indicates carbonate and siliciclastics with and without glacial features from top to base. Sta—Santa; MJ—Jacadigo hill; TQ—Taquaral hill; DL—Divina Luz farm; SC—São Carlos farm; CP—Córrego das Pedras; RAB19—drill core from Rabicho hill; MAR—Marinha (Navy) area; NR—Northern Rabicho. See the Supplemental Material for columnar sections (see footnote 1).

(Frei et al., 2017). The $^{40}Ar/^{39}Ar$ geochronology of cryptomelane established a minimum age of 587 ± 7 Ma for the group (Piacentini et al., 2013). The Jacadigo Group is overlain by late Ediacaran carbonates of the Corumbá Group (Fig. 1; Gaucher et al., 2003; Parry et al., 2017).

JACADIGO RECORD

Detailed field mapping and stratigraphic logging (Figs. S1–S5 in the Supplemental Material[1]), stable isotope analyses (Figs. S6 and S7, Tables S1 and S2), and detrital zircon geochronology (Figs. S8–S12, Table S3) in and around the UD allowed interpretation and global correlation of previously unrecognized sedimentary sequences within the Jacadigo Group. The resultant sequence stratigraphic framework for

the Jacadigo Group (Fig. 1) consists of lower and upper sequences recording major glacioeustatic fluctuations, postglacial carbon and oxygen isotope excursions (Fig. 2), and provenance evolution (Fig. 3) that fit the extreme environmental changes known for the Cryogenian.

The lower sequence (S1), part of the Urucum Formation, overlies basement rocks and is overlain by siliciclastic deposits of sequence S2 in the northern UD (Figs. 1 and 2; Fig. S1). At its base, S1 is dominated by monomictic pebble- to boulder-grade breccia with subordinate conglomeratic arkose and diamictite (Figs. 2A and 2B). Basement fractures immediately beneath the Urucum Formation locally exhibit long, decimeter- to meter-scale, subvertical, wedge-shaped, poorly sorted, angular sediment fillings (Figs. S2A–S2C), interpreted as frost wedges (sensu Eyles and Eyles, 2010). Clasts present a fitted fabric just above the contact, but they also occur locally in sigmoidal clusters, which may include grooved clasts (Fig. 4A; Figs. S2F and S2G). These features are interpreted as the

product of glaciotectonic shear of ice-cemented clasts on a frost-riven basement (Williams and Tonkin, 1985; Czudek, 1995; Passchier et al., 1998). Bullet-shaped boulders (Fig. 4B) also suggest glacial erosion (Clark and Hansel, 1989).

Dolostone up to 100 m thick conformably overlies basal breccias of sequence S1 and is locally topped by diamictite (Fig. 1; Figs. S1D, S2A, and S2B). The dolostone beds are dominated by superimposed centimeter- to meter-scale wave ripples, as well as low-angle cross-strata with minor stromatolitic intercalations, some containing acritarchs (Figs. S3A and S3B). The $\delta^{13}C$ values for these transgressive marine shelf deposits vary from 0 to +8.5‰ (Fig. 2), similar to the Cryogenian interglacial Keele peak positive excursion (Halverson and Shields-Zhou, 2011; Fig. S7).

The carbonate succession of S1 thickens to the southeast to ~650 m, but it terminates in an erosional unconformity (Figs. 1 and 2) exhibiting local paleokarstic dissolution features (Fig. 4C). The thickness and position of this
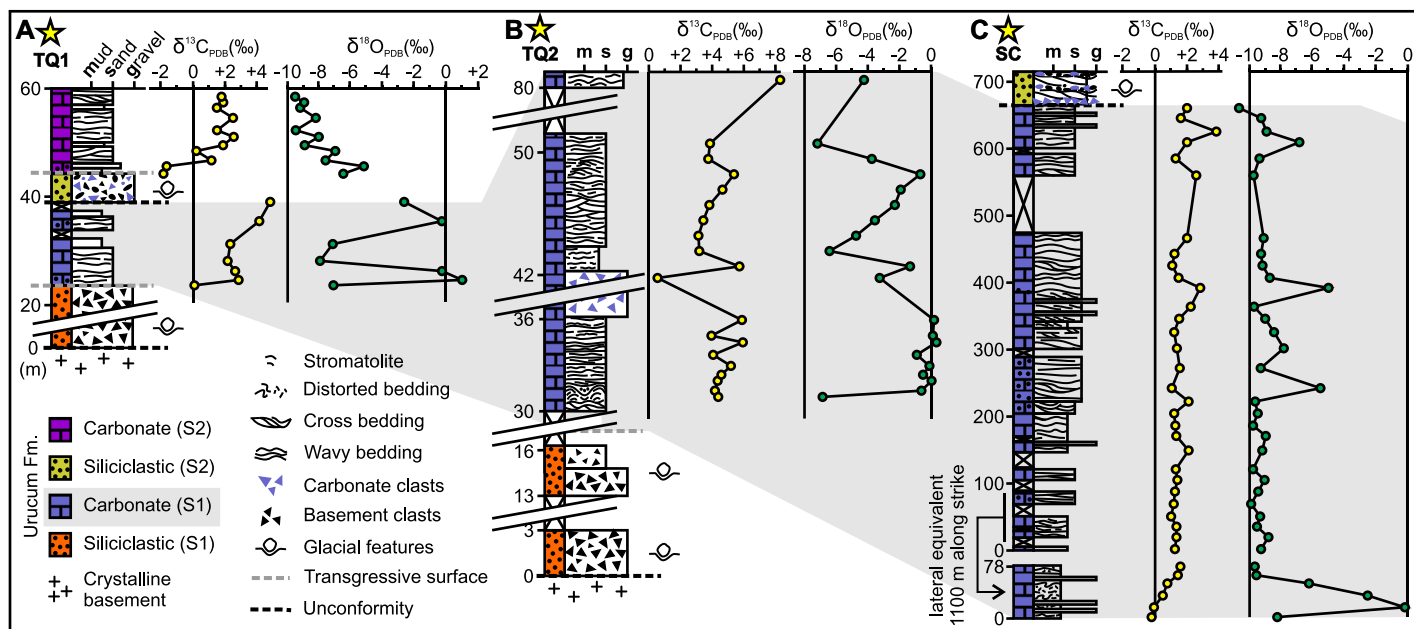
Figure 2. Chemostratigraphic correlation of studied successions across the basin. PDB—Peedee belemnite standard.

succession imply that the stratigraphic thickness in the Jacadigo Group varies less than 1 km over more than 15 km distance from central UD to the northwest and southeast (Fig. S1C). This carbonate succession is dominated by locally impure cross-bedded grainstone, often organized in meter-scale fining-upward cycles (Fig. S3C). Meter-scale lenses of carbonate breccia displaying ooid grainstone and stromatolite clasts are intercalated along the succession, especially at the base, where they are often associated with fine-grained facies locally displaying vase-shaped microfossils (VSMs) and soft sediment deformation (Figs. S3D and S3F). The S1 dolostone formed on a carbonate platform, thickening and then pinching out to the southeast at the shelf to slope transition. The $\delta^{13}C$ values range from $-0.2‰$ to $+4‰$, in a positive excursion (Fig. 2) consistent with deposition of the carbonate platform during the Cryogenian interglacial transgression (Fig. SF7), followed by glacioeustatic sea-level fall, and subsequent exposure and incision, as interpreted from paleokarst and paleovalleys associated with the regional unconformity at the top of S1.

The upper sequence (S2) comprises siliciclastic successions of the Urucum Formation and conformable overlying carbonates, as well as the IF-dominated succession of the Santa Cruz Formation. Basal siliciclastic strata of S2 onlap the glacioeustatic unconformity or conformably overlie the merged unconformities at the top of the basement (Fig. 1). In the Urucum Formation, coarse-grained deposits of S2 can be readily distinguished from those of S1 by their polymictic character, which includes abundant carbonate clasts that display distinct detrital zircon provenance (Fig. 3), stable isotope signatures (Table S1), and microfossil content (Fig.

S1E and S1F) that identify them as derived from S1 carbonate beds.

Basal siliciclastic deposits of S2 are mostly diamictite, locally Fe-rich, and up to a few tens of meters thick in the northern study area (Figs. 1, 2A, and 2C). These facies and correlative breccia exhibit evidence of glacial sedimentation, like abundant faceted, shattered, and plastically deformed clasts, as well as rare, striated boulders (Benn and Evans, 2014; Figs. S4A–S4D).

Conformably overlying, proximal coarse-grained basal deposits of S2 are a few tens of meters of carbonate dominated by grainstone, locally presenting trough and low-angle cross-strata (Fig. 2A). These facies display varied degrees of silicification and Fe enrichment, being at some places completely obliterated by cryptocrystalline hematite and jasper (Fig. S5D). The $\delta^{13}C$ profile records a positive excursion from $-2‰$ to $+3‰$ (Fig. 2A), comparable to that of transgressive post-Marinoan carbonate successions (Halverson and Shields-Zhou, 2011; Fig. S7).

In the center of the UD, where the Jacadigo Group is thickest, the base of S2 is dominated by sandy heterolithic deposits of the Urucum Formation up to 450 m thick, with plenty of meter-scale wave strata and minor swaley and hummocky structures (Fig. S5A), interpreted as offshore-transition storm-influenced facies deposited during eustatic fall and glacial advance at higher latitudes. In drill cores, pyritized VSM-bearing black shales (Fig. S5B) are succeeded by sandstone at the top of the Urucum Formation, prior to massive IF deposition (Fig. 1; Fig. S1).

The upper sandstone of the Urucum Formation, mappable in most of the UD hills, onlaps

the unconformity at the top of the S1 carbonate succession (Figs. 1 and 2C; Fig. S1). These deposits are poorly sorted, graded beds intercalated with breccia, and they display polymictic outsized clasts (Fig. 4D), cross-stratification, and wave ripples. They are interpreted as forced regressive deposits of glacial outwash deltas onlapping the carbonate platform to present-day northwest (Fig. 1). In this context, intraformational sandstone clasts (Fig. 4E; Figs. S4C and S5C) are interpreted as ice-cemented clasts (Waller et al., 2009; Runkel et al., 2010) derived from adjacent outwash plains.

Up section, the IF-dominated succession of the Santa Cruz Formation features outsized lonestones, often composed of granite and locally of diamictite, with some displaying disrupted beds below (Fig. 4F; Fig. S5E). These are interpreted as dropstones, including clasts of ice-cemented till (Chumakov, 2015). Discrete horizons of scattered angular and poorly sorted sand grains to granules represent glacial rainout (Chumakov, 2015; Fig. S5F).

Detrital Zircon Provenance

We present 911 new U-Pb laser ablation–inductively coupled plasma–mass spectrometry (LA-ICP-MS) detrital zircon ages from eight samples of the Urucum Formation (Figs. S8 and S9), added to 145 previous ages from two other samples (McGee et al., 2018) and 46 new U-Pb sensitive high-resolution ion microprobe (SHRIMP) ages of zircon grains from VSM-bearing carbonate clasts (Fig. 3; Figs. S10 and S11). The data set, as well as all individual samples, shows a marked age cluster between 1900 and 1700 Ma (81% of data set), corresponding to the age of adjacent basement rocks, with minor populations of Mesoproterozoic to
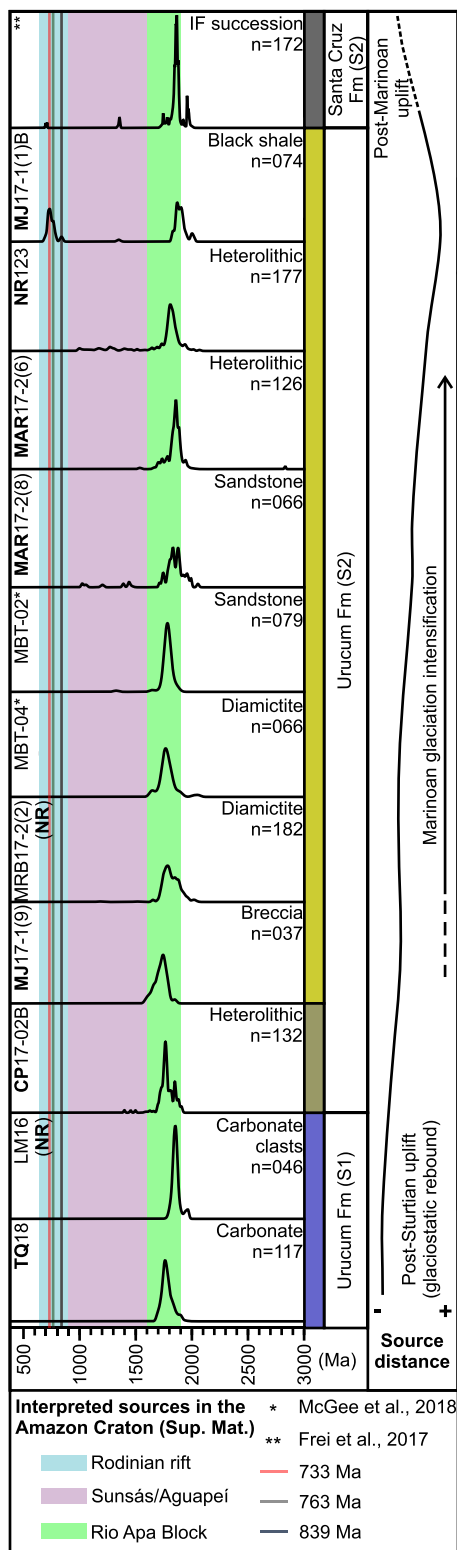
Figure 3. Probability density plots for detrital zircon U-Pb ages in lower and upper sequences of the Jacadigo Group, Brazil. Sample field codes and stratigraphy color scheme as in Figure 1. IF—iron formation. See sample details in the Supplemental Material (see footnote 1).

early Tonian (4%) and Paleoproterozoic (8%) ages sourced in the nearby Amazon craton (Fig. 3; Fig. S12). One sample from the VSM-bearing black shale at the top of the Urucum Formation (Fig. 3; Fig. S1F) provided two age clusters: one the age of adjacent basement and the other ca. 740 Ma (3% of data set; Fig. 3). The latter population, also evident in the Santa Cruz Formation (Frei et al., 2017), contained two Cryogenian-aged grains, the youngest of which was dated at 690 ± 18 Ma. It likely came from distant uplifted rifted Rodinian magmatic rocks at the margin of the Amazon craton (Manoel et al., 2021). These younger zircon grains found in a sample from sequence S2 (Fig. 3) do not rule out a Sturtian age for this sequence. However, the stratigraphic framework and associated provenance evolution reported here are better reconciled with two major glacial episodes than to multiple ice ages within a single cryochron.

The striking dominance of an adjacent basement source for zircon in both S1 carbonates and most S2 siliciclastics is attributed to glaciostatic uplift following Sturtian deglaciation (Fig. 3). A tectonic control for this source dominance is unlikely, as the stratigraphic architecture of the Jacadigo Group and facies distribution reported here challenge previous interpretations of marked tectonic uplift of basin margins.

The restriction of the remarkable Neoproterozoic age cluster to the upper siliciclastic succession in S2 (in addition to that previously observed in the Santa Cruz Formation) may reflect sediment transport along the widened drainage basins following post-Sturtian rebound and denudation (Fig. 3). Marinoan glacial advance over these basins may have transported Fe and Mn from the Stenian large igneous province in eastern Bolivia (Teixeira et al., 2015) to the Santa Cruz IFs.

DISCUSSION AND CONCLUSIONS

Previously unrecognized successions of the Urucum Formation completely change our understanding of the Jacadigo Group in the context of Cryogenian environmental evolution. Besides revealing the dominance of marine settings for most of Jacadigo Group deposition, detailed investigation of coarse-grained facies indicates glacial influence in two distinct intervals separated by a thick interglacial carbonate succession and a major unconformity. The gradual stratigraphic thickness variations of the Jacadigo Group, implicit in the recognition of the thick carbonate succession in S1, is better reconciled with deposition in a relatively smooth trough on a continental margin than within a fault-bounded rift basin. These thick transgressive and relatively ^{13}C-enriched carbonates ($\sim$+5‰ to 8‰) can be correlated with Cryogenian interglacial deposits worldwide (Halverson and Shields-Zhou, 2011). Detrital zircon ages in carbonate samples, including VSM-bearing clasts, indicate nearby basement as the dominant source, likely due to glaciostatic rebound.

Onset of a new glacial episode brought eustatic sea-level fall, and exposure and incision of the carbonate platform and adjacent basement, providing carbonate clasts and 1.9–1.7 Ga zircon grains to the main siliciclastic succession of the Urucum Formation. Latitudinal glacial advance was probably coeval with deposition of the thick storm-influenced marine strata above the glacioeustatic unconformity, yet still sourced from adjacent basement.

Younger age populations in VSM-bearing black shale record an expansion of provenance into Tonian to Sturtian sources, probably also reaching the Stenian large igneous province (Teixeira et al., 2015) of the southern Amazon craton. Subglacial fluxes leaching crushed metal-rich material along these regional-scale drainage basins were likely important sources for Fe and Mn buildup in the UD basin. Deglaciation under the high-CO$_2$ last stages of a second snowball Earth episode (Benn et al., 2015) resulted in massive deposition of Fe and Mn, as well as in the increased proximal signature in the detrital zircon provenance of the Santa Cruz Formation, reflecting a second glaciostatic rebound cycle.

This stratigraphic framework and sedimentary evolution prior to 587 ± 7 Ma, supported by carbon isotope excursions and detrital zircon provenance analysis, match Sturtian to Marinoan environmental changes. Our results imply that the largest Neoproterozoic IF is in fact Marinoan in age and that diachronism in Neoproterozoic IF deposition was controlled by the local interplay among source area composition, drainage basin evolution, glacioeustasy, and isostasy.

REFERENCES CITED
Angerer, T., Hagemann, S.G., Walde, D.H.G., Halverson, G.P., and Boyce, A.J., 2016, Multiple metal sources in the glaciomarine facies of the Neoproterozoic Jacadigo iron formation in the "Santa Cruz deposit," Corumbá, Brazil: Precambrian Research, v. 275, p. 369–393, https://doi.org/10.1016/j.precamres.2016.01.002.
Benn, D., and Evans, D.J.A., 2014, Glaciers and Glaciation (2nd ed.): London, Routledge, 817 p., https://doi.org/10.4324/9780203785010.
Benn, D.I., Le Hir, G., Bao, H., Donnadieu, Y., Dumas, C., Fleming, E.J., Hambrey, M.J., McMillan, E.A., Petronis, M.S., Ramstein, G., Stevenson, C.T.E., Wynn, P.M., and Fairchild, I.J., 2015, Orbitally forced ice sheet fluctuations during the Marinoan snowball Earth glaciation:
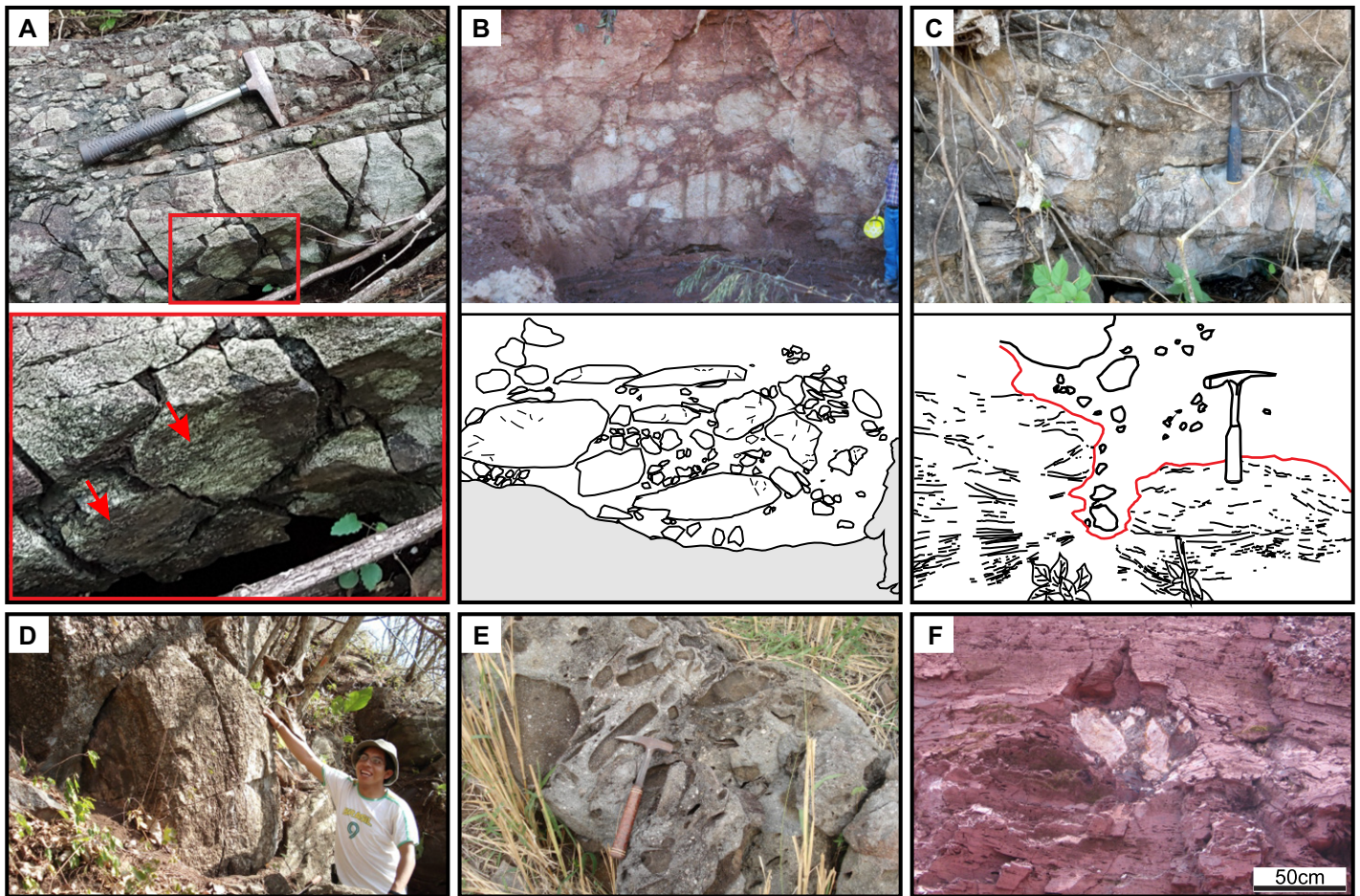
Figure 4. Key sedimentary features in the Jacadigo Group, Brazil. (A) Oblique view of sigmoidal clusters of fitted clasts; grooves in detail (red arrows). (B) Bullet-shaped clasts in basal boulder breccia and graphic interpretation. (C) Irregular surface separating cross-bedded carbonate and conglomeratic sandstone with graphic interpretation. (D) Outsized carbonate boulder on disrupted sandstone bed. (E) Intraformational sandstone breccia. (F) Diamictite boulder disrupting bedding within banded iron formation.

Nature Geoscience, v. 8, p. 704–707, https://doi.org/10.1038/ngeo2502.

Chumakov, N.M., 2015, Problem of the identification of ancient glacial sediments: Lithology and Mineral Resources, v. 50, p. 134–143, https://doi.org/10.1134/S0024490215010022.

Clark, P.U., and Hansel, A.K., 1989, Clast ploughing, lodgement and glacier sliding over a soft glacier bed: Boreas, v. 18, p. 201–207, https://doi.org/10.1111/j.1502-3885.1989.tb00392.x.

Cox, G.M., Halverson, G.P., Minarik, W.G., Le Heron, D.P., Macdonald, F.A., Bellefroid, E.J., and Strauss, J.V., 2013, Neoproterozoic iron formation: An evaluation of its temporal, environmental and tectonic significance: Chemical Geology, v. 362, p. 232–249, https://doi.org/10.1016/j.chemgeo.2013.08.002.

Cox, G.M., Halverson, G.P., Poirier, A., Le Heron, D., Strauss, J.V., and Stevenson, R., 2016, A model for Cryogenian iron formation: Earth and Planetary Science Letters, v. 433, p. 280–292, https://doi.org/10.1016/j.epsl.2015.11.003.

Cox, G.M., Isakson, V., Hoffman, P.F., Gernon, T.M., Schmitz, M.D., Shahin, S., Collins, A.S., Preiss, W., Blades, M.L., Mitchell, R.N., and Nordsvan, A., 2018, South Australian U-Pb zircon (CA-ID-TIMS) age supports globally synchronous Sturtian deglaciation: Precambrian Research, v. 315, p. 257–263, https://doi.org/10.1016/j.precamres.2018.07.007.

Czudek, T., 1995, Cryoplanation terraces—A brief review and some remarks: Geografiska Annaler

A: Physical Geography, v. 77, p. 95–105, https://doi.org/10.1080/04353676.1995.11880431.

de Almeida, F.F.M., 1946, Origem dos minérios de ferro e manganês de urucum, Corumbá, Estado de Mato Grosso: Rio de Janeiro, Brazil, Departamento Nacional da Produção Mineral Boletin 119, 58 p.

Eyles, C.H., and Eyles, N., 2010, Glacial deposits, in James, N.P., and Dalrymple, R.W., eds., Facies Models 4: Geological Association of Canada GeoText 6, p. 73–104.

Frei, R., Døssing, L.N., Gaucher, C., Boggiani, P.C., Frei, K.M., Bech Árting, T., Crowe, S.A., and Freitas, B.T., 2017, Extensive oxidative weathering in the aftermath of a late Neoproterozoic glaciation—Evidence from trace element and chromium isotope records in the Urucum District (Jacadigo Group) and Puga iron formations (Mato Grosso do Sul, Brazil): Gondwana Research, v. 49, p. 1–20, https://doi.org/10.1016/j.gr.2017.05.003.

Freitas, B.T., Warren, L.V., Boggiani, P.C., Almeida, R.P., and Piacentini, T., 2011, Tectono-sedimentary evolution of the Neoproterozoic BIF-bearing Jacadigo Group, SW-Brazil: Sedimentary Geology, v. 238, p. 48–70, https://doi.org/10.1016/j.sedgeo.2011.04.001.

Gaucher, C., Boggiani, P.C., Sprechmann, P., Sial, A.N., and Fairchild, T.R., 2003, Integrated correlation of the Vendian to Cambrian Arroyo del Soldado and Corumbá Groups (Uruguay and Brazil):

Palaeogeographic, palaeoclimatic and palaeobiologic implications: Precambrian Research, v. 120, p. 241–278, https://doi.org/10.1016/S0301-9268(02)00140-7.

Halverson, G.P., and Shields-Zhou, G., 2011, Chemostratigraphy and the Neoproterozoic glaciations, in Arnaud, E.A., Halverson, G.P., and Shields-Zhou, G., eds., The Geological Record of Neoproterozoic Glaciations: Geological Society [London] Memoir 36, p. 51–66, https://doi.org/10.1144/M36.4.

Manoel, T.N., Selby, D., Galvez, M.E., Leite, J.A.D., and Figueiredo, L.N., 2021, A pre-Sturtian depositional age of the lower Paraguay belt, western Brazil, and its relationship to western Gondwana magmatism: Gondwana Research, v. 89, p. 238–246, https://doi.org/10.1016/j.gr.2020.10.002.

McGee, B., Babinski, M., Trindade, R.I.F., and Collins, A.S., 2018, Tracing final Gondwana assembly: Age and provenance of key stratigraphic units in the southern Paraguay belt, Brazil: Precambrian Research, v. 307, p. 1–33, https://doi.org/10.1016/j.precamres.2017.12.030.

Nelson, L.L., Smith, E.F., Hodgin, E.B., Crowley, J.L., Schmitz, M.D., and Macdonald, F.A., 2020, Geochronological constraints on Neoproterozoic rifting and onset of the Marinoan glaciation from the Kingston Peak Formation in Death Valley, California (USA): Geology, v. 48, p. 1083–1087, https://doi.org/10.1130/G47668.1.

Parry, L.A., Boggiani, P.C., Condon, D.J., Garwood, R.J., Leme, J.M., McIlroy, D., Brasier, M.D., Trindade, R.I.F., Campanha, G.A.C., Pacheco, M.L.A.F., Diniz, C.Q.C., and Liu, A.G., 2017, Ichnological evidence for meiofaunal bilaterians from the terminal Ediacaran and earliest Cambrian of Brazil: Nature Ecology & Evolution, v. 1, p. 1455, https://doi.org/10.1038/s41559-017-0301-9.

Passchier, S., Wilson, T.J., and Paulsen, T.S., 1998, Origin of breccias in the CRP-1 core: Terra Antartica, v. 5, p. 401–409.

Piacentini, T., Vasconcelos, P.M., and Farley, K.A., 2013, ^{40}Ar/^{39}Ar constraints on the age and thermal history of the Urucum Neoproterozoic banded iron-formation, Brazil: Precambrian Research, v. 228, p. 48–62, https://doi.org/10.1016/j.precamres.2013.01.002.

Redes, L.A., de Sousa, M.Z.A., Ruiz, A.S., and Lafon, J.-M., 2015, Petrogenesis and U-Pb and Sm-Nd geochronology of the Taquaral granite: Record of an orosirian continental magmatic arc in the region of Corumba, MS: Brazilian Journal of Geology, v. 45, p. 431–451, https://doi.org/10.1590/2317-488920150030231.

Rooney, A.D., Yang, C., Condon, D.J., Zhu, M., and Macdonald, F.A., 2020, U-Pb and Re-Os geochronology tracks stratigraphic condensation in the Sturtian snowball Earth aftermath: Geology, v. 48, p. 625–629, https://doi.org/10.1130/G47246.1.

Runkel, A.C., Mackey, T.J., Cowan, C.A., and Fox, D.L., 2010, Tropical shoreline ice in the late Cambrian: Implications for Earth's climate between the Cambrian Explosion and the Great Ordovician Biodiversification Event: GSA Today, v. 20, no. 11, p. 4–10, https://doi.org/10.1130/GSATG84A.1.

Teixeira, W., Hamilton, M.A., Lima, G.A., Ruiz, A.S., Matos, R., and Ernst, R.E., 2015, Precise ID-TIMS U-Pb baddeleyite ages (1110–1112 Ma) for the Rincón del Tigre–Huanchaca large igneous province (LIP) of the Amazonian craton: Implications for the Rodinia supercontinent: Precambrian Research, v. 265, p. 273–285, https://doi.org/10.1016/j.precamres.2014.07.006.

Trompette, R., de Alvarenga, C.J.S., and Walde, D., 1998, Geological evolution of the Neoproterozoic Corumbá graben system (Brazil): Depositional context of the stratified Fe and Mn ores of the Jacadigo Group: Journal of South American Earth Sciences, v. 11, p. 587–597, https://doi.org/10.1016/S0895-9811(98)00036-4.

Urban, H., Stribrny, B., and Lippolt, H.J., 1992, Iron and manganese deposits of the Urucum District, Mato Grosso do Sul, Brazil: Economic Geology and the Bulletin of the Society of Economic Geologists, v. 87, p. 1375–1392, https://doi.org/10.2113/gsecongeo.87.5.1375.

Waller, R., Murton, J., and Whiteman, C., 2009, Geological evidence for subglacial deformation of Pleistocene permafrost: Proceedings of the Geologists' Association, v. 120, p. 155–162, https://doi.org/10.1016/j.pgeola.2009.08.009.

Williams, G.E., and Tonkin, D.G., 1985, Periglacial structures and palaeoclimatic significance of a late Precambrian block field in the Cattle Grid copper mine, Mount Gunson, South Australia: Australian Journal of Earth Sciences, v. 32, p. 287–300, https://doi.org/10.1080/08120098508729331.

Zhou, C., Huyskens, M.H., Lang, X., Xiao, S., and Yin, Q.-Z., 2019, Calibrating the terminations of Cryogenian global glaciations: Geology, v. 47, p. 251–254, https://doi.org/10.1130/G45719.1.

Printed in USA